Inorganic Chemistry

Article

pubs.acs.org/IC

Surface Modification of Al_{30} Keggin-Type Polyaluminum Molecular Clusters

Samangi Abeysinghe, Daniel K. Unruh, and Tori Z. Forbes*

Department of Chemistry, University of Iowa, W374 Chemistry Building, Iowa City, Iowa 52242, United States

Supporting Information

ABSTRACT: Keggin-type molecular clusters formed from the partial hydrolysis of aluminum in aqueous solutions have the capacity to adsorb a variety of inorganic and organic contaminants. The adsorptive capability of Keggin-type polyaluminum species, such as Al_{13} and Al_{30}, lead to their wide usage as precursors for heterogeneous catalysts and clarifying agents for water purification applications, but a molecular-level understanding of adsorption process is lacking. Two model Al_{30} clusters, whose surface has been modified with chelated metals (Al^{3+} and Zn^{2+}) have been synthesized and structurally characterized by single-crystal X-ray diffraction. **Al_{32}IDA** $[(Al(IDA)H_2O)_2(Al_{30}O_8(OH)_{60}(H_2O)_{22})](2,6\text{-NDS})_4(SO_4)_2Cl_4(H_2O)_{40}$, IDA = iminodiacetic acid, 2,6-NDS = 2,6 napthalene disulfonate) crystallize in the triclinic space group, $P\bar{1}$ with a = 13.952(2) Å, b = 16.319(3) Å, c = 23.056(4) Å, α = 93.31(1)°, β = 105.27(1)°, and γ = 105.52(1)°. **Zn_2Al_{32}** $[(Zn(NTA)H_2O)_2(Al(NTA)(OH)_2)_2(Al_{30}(OH)_{60}(O)_8(H_2O)_{20}](2,6\text{-NDS})_5(H_2O)_{64}$, (NTA = nitrilotriacetic acid), also crystallizes in $P\bar{1}$ with unit cell parameter refined as a = 16.733(7) Å, b = 18.034(10) Å, c = 21.925(11) Å, α = 82.82(2)°, β = 70.96(2)°, and γ = 65.36(2)°. The chelated metal centers adsorb to the surface of the Al_{30} clusters through hydroxyl bridges located at the central belt region of the molecule. The observed binding sites for the metal centers mirror the reactivity predicted by previously reported molecular dynamic simulations and can be identified by the acidity and hydration factor of the water group that participates in the adsorption process.

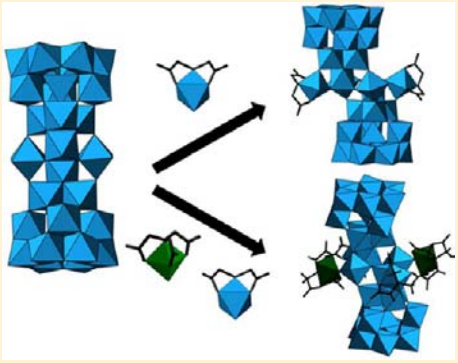

INTRODUCTION

The formation of crystalline and colloidal aluminum oxide and hydroxide compounds is controlled by the hydrolysis of the Al^{3+} cation in aqueous solution.[1−5] Aquo complexes ($Al(OH_2)_6]^{3+}$) form upon dissolution of the metal and behave as a hard Lewis acid, forming a series of soluble hydroxylated species.[6] Potentiometric and NMR techniques have identified several of these smaller condensation products, including monomeric $(AlOH)^{2+}$, $(Al(OH)_2)^{+}$, $(Al(OH)_4)^{-}$, dimeric $(Al_2(OH)_2)^{4+}$, and trimeric $(Al_3(OH)_4)^{5+}$ complexes.[7−11] Larger Al_{13} tridecamers $(Al_{13}O_4(OH)_{24})^{7+}$ displaying a Baker−Figgis−Keggin or Keggin-type structural arrangement dominate in partially hydrolyzed aqueous solutions when the hydroxylation rate is increased substantially via titration with a hard base.[7] Upon aging or additional heating, the tridecameric species can polymerize into larger polyaluminum clusters, such as the Al_{30} cluster $(Al_{30}O_8(OH)_{56}(H_2O)_{24}]^{18+}$, that account for up to 80% of the aluminum cations present in these solutions.[12,13]

Aluminum hydrolysis products have a wide range of industrial uses, but the high propensity of the Keggin-type polyaluminum clusters to adsorb organic and inorganic species makes them especially useful as precursors for heterometallic catalysts[14] and clarifying agents for water purification applications.[15] Their ability to adsorb a variety of organic and inorganic constituents on the surface of the Keggin-type polyaluminum species is related to the deprotonation of amphoteric functional groups. Removal of H atoms from nonbridging water molecules located on the outer vertices of the ε-Al_{13} molecule begins at pH 6 and forms discrete positively charged species (Al_{13}^{5+}, Al_{13}^{3+}, and Al_{13}^{+}) over a narrow pH range.[16] The resulting titration curve for ε-Al_{13} is remarkably steep because of the loss of three protons per cluster over the course of 0.2 units in a dilute solution.[16,17] Similar results were obtained for the Al_{30} cluster, although the slope of the titration curve is more gradual and the initial deprotonation events are more defined.[18] At a pH of approximately 5.5, the Al_{30} ion loses 2.3 protons, but subsequent neutralization of the cluster does not occur until the solution pH reaches 6.7.[18]

Deprotonation of the surface bound water molecules of the polyaluminum clusters creates hydroxyl groups that possessed a high affinity for metal cations, such as copper, nickel, and zinc.[19−23] Between a pH of 5.5−6.1, metals adsorbed to the surface of the ε-Al_{13} or Al_{30} clusters, forming soluble complexes in aqueous solutions.[22] In more alkaline regions, precipitation of the polyaluminum complexes occurs, effectively removing the dissolved metals from the solution and forming the basis for the flocculation mechanism used in water purification processes.[21] Organic molecules with hydroxyl or carboxylate

Received: February 6, 2013
Published: April 30, 2013

   dx.doi.org/10.1021/ic400321k | Inorg. Chem. 2013, 52, 5991−5999

functional groups also strongly chelate the aluminum cation and can be removed from the water column via a similar adsorption/flocculation phenomena.[24,25]

The adsorption of transition metals and organic species by the Keggin-type clusters has been investigated using bulk adsorption experiments and spectroscopic techniques, but an exact molecular level understanding of the possible binding sites is lacking.[20,22] Molecular dynamic simulations have provided information regarding possible deprotonation scenarios,[26] but currently there is little experimental evidence available to link these studies to absorption processes. Herein, we present the synthesis and structural characterization of Al_{30} model clusters that have been modified by chelated metal centers (**Al_{32}IDA** = $[(Al(IDA)H_2O)_2(Al_{30}O_8(OH)_{60}(H_2O)_{22})](2,6\text{-NDS})_4(SO_4)_2Cl_4(H_2O)_{40}$, IDA = iminodiacetic acid, 2,6-NDS = 2,6 napthalene disulfonate) and **Zn_2Al_{32}NTA** = $[(Zn(NTA)H_2O)_2(Al(NTA)(OH)_2)_2(Al_{30}(OH)_{60}(O)_8(H_2O)_{20}](2,6\text{-NDS})_5(H_2O)_{64}$, (NTA = nitrilotriacetic acid) and provide structural and chemical characterization of the compounds. These compounds serve as molecular models to provide additional information regarding the preferred adsorption sites on the Al_{30} species and can be compared to previously reported molecular dynamics simulations.[26]

EXPERIMENTAL SECTION

Syntheses. The reagents $AlCl_3{\cdot}6H_2O$ (Fisher Scientific 7784-13-6), NaOH (Fisher Scientific 1310-73-2), 2,6-naphthalene disulfonic acid disodium salt (2,6-NDS) (MP Biomedical 1655-45-4), iminodiacetic acid (IDA) (98%, Fluka Analytical 142-73-4), zinc chloride (Fisher Scientific 7646-85-7), and nitrilotriacetic acid (Sigma Aldrich 5064-31-3) were used as received. The reactions were carried out in Teflon lined Parr bombs with 23 mL internal volume. An initial partially hydrolyzed aluminum stock solution was prepared by heating 25 mL of a 0.25 M $AlCl_3$ (6.25 mmol) solution to 80 °C in a water bath, followed by a dropwise addition of 60 mL of 0.25 M NaOH (6.25 mmol) to a hydrolysis ratio (OH^-/Al^{3+}) of 2.4. The Al_{13} stock was cooled to room temperature and used within one week from the initial solution preparation.

Al_{32}IDA was synthesized by adding 0.0312 g of sodium iminodiacetate to 7 mL of the Al_{13} stock solution, and the reactants were stirred at room temperature for 20 min. After total dissolution of the iminodiacetate salt, the clear solution was loaded into a 23-mL Teflon-lined Parr acid digestion vessel and heated at 80 °C for 24 h in a gravimetric oven to encourage the formation of the larger polyaluminum species. The resulting solution was cooled to room temperature, transferred into a glass vial, and 3 mL of 0.1 M 2,6-NDS (2,6-NDS = 2,6 napthalene disulfonate) was added to induce crystallization. Colorless plate-like crystals formed from slow evaporation of the solution for approximately 12 days that were suitable for single crystal X-ray diffraction studies. Approximate percent yield of the **Al_{32}IDA** was 23% based upon Al.

Zn_2Al_{32}NTA was formed by adding 0.0308 g of $ZnCl_2$ and 0.0345 g of nitrilotriacetic acid (NTA) to 7 mL of the Al_{13} stock solution. Again, the mixture was stirred for 20 min, loaded in to a Teflon-lined Parr reaction vessel, and reacted for 24 h at 80 °C. After heating, the solution was cooled to room temperature, transferred to a 23 mL scintillation vial, and 3 mL of a 0.1 M 2,6-NDS were added as the crystallizing agent. The contents were mixed and the solution was allowed to slowly evaporate for 21 days. At that time, colorless blocky crystals formed on the bottom of the glass vial with approximately 9% yields based upon Al.

Single-Crystal X-ray Diffraction. Crystals were isolated from the mother liquor and mounted on a Bruker Nonius KappaCCD single crystal X-ray diffractometer equipped with MoKα radiation (λ = 0.7107 Å) and a low temperature cryostat. Data collection, cell refinement, data reduction, and absorption corrections were performed using Collect[27] and HKL Scalepack/Denzo[28] software. Structure solutions were performed using direct methods and refined on the basis of F^2 for all unique data using the Bruker SHELXTL[29] version 5 system of programs. Atomic scattering factors for each atom were taken from the International Tables of X-ray Crystallography.[30] Selected data collection parameters and crystallographic information are provided in Table 1.

Table 1. Selected Crystallographic Information for $((Al(IDA)H_2O)_2(Al_{30}O_8(OH)_{60}(H_2O)_{22})(2,6\text{-NDS})_4(SO_4)_2Cl_4(H_2O)_{40}$ (Al_{32}IDA) and $[(Zn(NTA)H_2O)_2(Al(NTA)(\mu_2\text{-OH})_2)_2(Al_{30}(\mu_2\text{-OH})_{54}(\mu_3\text{-OH})_6(\mu_4\text{-O})_8(H_2O)_{20}(2,6\text{-NDS})_5(H_2O)_{64}]$ (Zn_2Al_{32}NTA)

	Al_{32}IDA	Zn_2Al_{32}NTA
FW (g/mol)	4902.5	6109.2
space group	$P\bar{1}$	$P\bar{1}$
a (Å)	13.952(2)	16.733(7)
b (Å)	16.319(3)	18.034(10)
c (Å)	23.056(4)	21.925(11)
α (°)	93.31(1)	82.821(19)
β (°)	105.27(1)	70.958(17)
γ (°)	105.52(1)	65.362(18)
V (Å^3)	4805.1(2)	5672(5)
Z	1	1
ρ_{calc} (g/cm^3)	1.020	1.359
μ (mm^{-3})	0.422	0.530
F(000)	2038	2322
crystal size (mm)	0.095 × 0.170 × 0.185	0.138 × 0.128 × 0.98
θ range	0.92 to 25.04°	0.98 to 26.07°
data collected	$-16 < h < 15$	$-20 < h < 20$
	$-19 < k < 19$	$-22 < k < 21$
	$0 < l < 27$	$-27 < l < 27$
completeness to θ = 25.04°	99.3%	98.2%
reflections collected/unique	16894/16894	81079/22035
GOF on F^2	0.998	1.123
final R indices [$I > 2\sigma(I)$]	R_1 = 0.0888,	R_1 = 0.0693,
	wR_2 = 0.2810	wR_2 = 0.2234
R indices (all data)	R_1 = 0.1026,	R_1 = 0.0797,
	wR_2 = 0.3019	wR_2 = 0.2364
largest diff. peak and hole (Å^3)	1.659 and −0.884	2.026 and −2.609

Al_{32}IDA crystallize in the triclinic space group, $P\bar{1}$, with a = 13.952(2) Å, b = 16.319(3) Å, c = 23.056(4) Å, α = 93.31(1)°, β = 105.27(1)°, and γ = 105.52(1)°. **Zn_2Al_{32}NTA** also crystallizes in the triclinic $P\bar{1}$ space group with unit cell parameter refined as a = 16.733(7) Å, b = 18.034(10) Å, c = 21.925(11) Å, α = 82.82(2)°, β = 70.96(2)°, and γ = 65.36(2)°. The Al, Zn, and S atoms were located in the direct methods solutions and the O and C atoms were identified in the difference Fourier maps calculated following refinement of the partial-structure models.

The Al, Zn, and O atoms associated with the polyaluminum clusters could be refined anisotropically, but structural disorder was prevalent for the disulfonate anions, organic chelators, and the solvent (H_2O) molecules. Disorder of the 2,6-NDS anion was caused by the free rotation about the S−C bond, leading to anisotropy of the electron density associated with the oxygen atoms of the sulfonate functional group. The sulfate anion (S5) in **Al_{32}IDA** was modeled as a split site with a refined occupancy of 70% and 30% for S5A and S5B, respectively. Disorder of the IDA molecule also required separation of several C and O atoms into two crystallographically distinct sites, each with 50% occupancy. The electron density for four oxygen atoms (O52, O53, O55, and O74) of the sulfonate groups in **Zn_2Al_{32}NTA** was also relatively diffuse; therefore, these atoms were modeled as split sites with 50% occupancy. The carbon atoms associated with the naphthalene ring of the 2,6-NDS molecule containing the S5 atom in

dx.doi.org/10.1021/ic400321k | Inorg. Chem. 2013, 52, 5991−5999

the **Zn_2Al_{32}NTA** compound were also disordered and modeled as split sites. Additional disordered solvent molecules (H_2O) present in the interstitial regions of both structures could not be resolved; therefore the diffuse electron density associated with the solvent molecules was modeled using the SQUEEZE command in the PLATON[31] software. Use of the SQUEEZE command reduced the R_1 value from 16.75% to 8.88% for **Al_{32}IDA** and 18.9 to 6.93% for **Zn_2Al_{32}NTA**.

Hydrogen positions for the naphthalene rings of the disulfonate anions and aliphatic backbone of the IDA and NTA molecules were placed using a riding model with a fixed C−H distance of 0.93 Å. Additional hydrogen bonds could not be located for the Al polycations because of the high levels of diffuse electron density associated with the disorder of solvent in the interstitial regions. Crystallographic information files (CIFs) for **Al_{32}IDA** and **Zn_2Al_{32}NTA** and additional bond distance tables can be found in the Supporting Information.

Characterization. *Powder X-ray Diffraction.* The synthesized compound were ground to a polycrystalline powder and analyzed on a Bruker D-5000 powder X-ray diffractometer (Cu Kα = 1.54 Å) equipped with a LynxEye solid state detector to determine purity of the sample. Scans were performed from 5 to 60° 2θ with a step size of 0.05° 2θ and a count time of 1 s/step. The experimental pattern was compared to predictions based upon the structure determination from single-crystal X-ray diffraction.

Infrared Spectroscopy. Approximately 5−10 mg of the powdered samples were mixed with anhydrous KBr salt and pressed into translucent discs. Infrared spectra for both materials were collected on a Nicolet Nexus FT-IR Spectrometer from 500 to 4000 cm^{-1}.

Chemical Composition. The elemental composition of each sample was verified using energy dispersive spectroscopy with a Hitachi 3400N Scanning Electron Microscope. Crystals were separated from the mother liquor and adhered to a SEM stub with double-sided carbon tape. The operating voltage and the emission current were 15.0 kV and 80−120 μA, respectively.

Zn_2Al_{32}NTA was also characterized by a Varian 720-ES ICP-OES instrument to confirm the presence of Zn on the polyaluminum clusters. A small quantity of the characterized powder was dissolved in a 2% nitric acid solution in triplicate. A standard curve was created in a similar matrix using 1000 ppm Zn standard purchase from Fisher Scientific. The experiment was performed on a Varian ICP-OES 720 system using the 202.548, 206.200, and 213.857 nm spectral emissions.

The hydration states of both compounds were determined using a TA Instruments Q500 thermogravimetric analyzer. Approximately 10−15 mg of the powdered sample was added to the aluminum pan and heated from 25 to 600 °C with a step rate of 5 °C/minute under dry air. The identity of the product after the heat cycle was determined using powder X-ray diffraction.

RESULTS AND DISCUSSION

Synthesis of Materials. Keggin-type polyaluminum species are difficult to crystallize as evidenced by the fact that over the past 50 years only a handful of clusters have been characterized by single-crystal X-ray diffraction.[9,12,13,32−36] The previously reported Al_{13}, Al_{30}, or Al_{32} polyaluminum clusters were successfully isolated by the addition of either sulfate or selenate anions, suggesting a favorable interaction that may aid in the crystallization process.[12,13,32−36] Given the large size, high charge, and prevalence of hydrogen bonding interactions by the Keggin-type clusters, a supramolecular approach was suggested as a novel route toward the characterization of new compounds.[9] This idea was previously applied using *p*-sulfonatocalix[4]arene and curcubit[6]uril, which did not result in the formation of new clusters, but was used to isolate the ε-Al_{13} and Al_{30} clusters.[34,35]

We have recently expanded this supramolecular approach toward the isolation of new compounds with the use of 2,6 napthalene disulfate as the crystallization agent.[36] These bulky anions can be paired with the large, highly charged (+16 to +18) polyaluminum clusters to provide a mechanism to enhance long-range ordering. Hydrogen bonding between the 2,6-NDS sulfonate functional groups and the polyaluminum species and $\pi-\pi$ stacking of the naphthalene rings increase the intramolecular interactions among the molecular constituents, effectively enhancing crystallization. In addition to **Al_{32}IDA** and **Zn_2Al_{32}NTA**, one new Keggin-type species (Al_{26}) has been previously isolated using 2,6-NDS as a crystallization agent.[36] This approach also improves upon the previously reported methods of the δ-Al_{13} and Al_{30} clusters, because these polyaluminum species can now be synthesized cleanly and in higher yields by simply varying the concentration of the 2,6-NDS in solution.[36]

Structural Description. The molecular species observed in both **Al_{32}IDA** and **Zn_2Al_{32}NTA** are based upon the Al_{30} Keggin-type cluster (Figure 1) that was first described by both Rowsell and Nazar[12] and Allouche[13] as the polymerization of two Al_{13} clusters. Each Al_{13} unit can be described as a central tetrahedrally coordinated Al atom surround by 12 additional Al atoms in octahedral coordination. The outer 12 Al atoms are arranged into 4 planar $Al_3(\mu_2\text{-}OH)_6(H_2O)_3$ (μ = bridging) trimers through edge sharing of hydroxyl groups. Each of the trimers are linked together through additional corner- and edge-sharing to form the $[Al(\mu_4\text{-}O_4)Al_{12}(\mu_2\text{-}OH)_{24}(H_2O)12]^{7+}$ polycation. The ε-Al_{13} Keggin-type structure, which is the most common isomer at low-temperatures, contains all four Al trimers bonded through edge-sharing of the hydroxyl groups. Rotation of one of the trimers by 60° results in shared-vertices and forms the δ-isomer. The mechanism and energetics for the conversion of the ε-Al_{13} to the δ-Al_{13} is unknown; however, several studies have previously suggested that δ-Al_{13} is a necessary building unit for the polymerization of the ε-Al_{13} Keggin molecule into larger polynuclear species.[3,32,36] Formation of the Al_{30} cluster occurs when two of the δ-Al_{13} moieties are joined through four octahedrally coordinated aluminum atoms located in a region commonly referred to as the central belt. The resulting polycation is approximately 2 nm in diameter and contains a variety of chemical environments available to adsorb inorganic and organic species.

The Al−O bond lengths observed for the Al_{30} molecule in the **Al_{32}IDA** and **Zn_2Al_{32}NTA** compounds are similar to those previously reported for the other Keggin-type polyaluminum species.[9,12,13,35,36] The central tetrahedrally coordinated Al atom is bonded to four oxygen atoms at distances ranging from 1.782(2)−1.833(3) Å and 1.787(3)−1.833(3) Å for **Al_{32}IDA** and **Zn_2Al_{32}NTA**, respectively. Octahedral coordination is also observed about the Al atoms via oxygen atoms, hydroxyl groups, or water molecules with bond lengths between 1.813(4) to 2.064(4) Å in both molecules.

Two additional chelated aluminum atoms are bonded to the exterior of the Al_{30} cluster in the **Al_{32}IDA** compound (Figure 1a). Iminodiacetic acid is a polyaminocarboxylate molecule ($^-OOCCH_2NHCH_2COO^-$) that chelates to the Al^{3+} cation in a tridentate fashion through the central amine group and carboxylate end members. The Al−N bond length (2.049(6) Å) is slightly longer than the Al−O distances associated with the carboxylate functional groups (1.896(5) and 1.896(5) Å). An additional water molecule is also bonded to the chelated Al atom at 1.907(5) Å, resulting in a relatively undistorted octahedral coordination about the metal center. Two of the chelated Al atoms coordinate to the surface of the Al_{30} cluster within the central belt region in a bridging bidentate fashion,

dx.doi.org/10.1021/ic400321k | Inorg. Chem. 2013, 52, 5991−5999

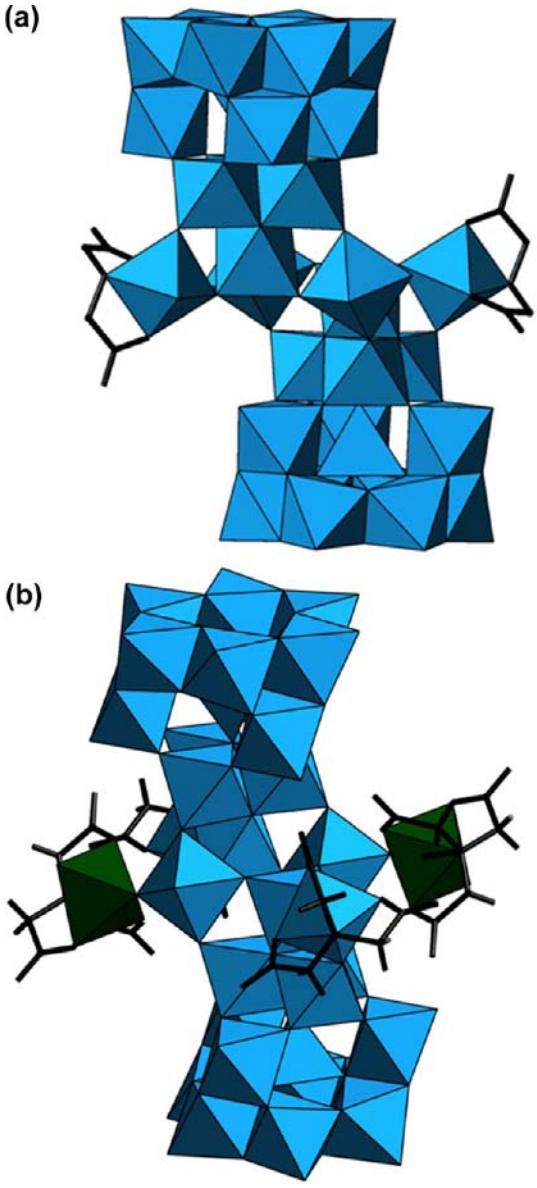

Figure 1. (a) $\mathbf{Al_{32}IDA}$ polycation built upon the Al_{30} Keggin-type species (Al atoms represented as blue polyhedra) with two additional chelated Al atoms bonded to the surface of the cluster. (b) $\mathbf{Zn_2Al_{32}NTA}$ contains a similar species with additional Al^{3+} (blue polyhedra) and Zn^{2+} atoms (green polyhedra) bonded to the Al_{30} polycation in the central belt region.

resulting in $[(Al(IDA)(H_2O))_2(Al_{30}O_8(OH)_{60}(H_2O)_{22})]^{16+}$ as the overall formula for the cluster.

The $\mathbf{Zn_2Al_{32}NTA}$ compound also contains the Al_{30} polycation, but has additional Al and Zn atoms adsorbed to the surface of the cluster (Figure 1b). Both metals are complexed by nitrilotriacetic acid ($N(CH_2COOH)_3$) in a tetradentate fashion through the carboxylate end members and the central amine group. The Al−O and Zn−O distances are observed from 1.868(3)−1.918(3) and 1.881(3)−2.068(4) Å, respectively, with slightly longer Al−N (2.113(3) Å) and Zn−N (2.149(3) Å) bond lengths. Each of the chelated metal cations are bonded to opposite sides of the Al_{30} molecule in the central belt region, although the coordination mode is different between the Zn and Al atoms. The Al^{3+} cations bond to the exterior of the cluster in a bridging-bidentate fashion and, along with the tetradentate chelation by the NTA molecule, result in an octahedral coordination geometry. Two Zn^{2+} atoms are also octahedrally coordinated via the NTA molecule, one additional water group, and a monodentate linkage to the Al_{30} cluster through the central belt region. The resulting polynuclear species has an overall formula of $[(Zn(NTA)(H_2O))_2(Al(NTA))_2(Al_{30}O_8(OH)_{58}(H_2O)_{22})]^{18+}$.

Three-dimensional molecular networks are formed by both $\mathbf{Al_{32}IDA}$ and $\mathbf{Zn_2Al_{32}NTA}$ compounds through hydrogen bonding between the polyaluminum clusters and napthalenedisulfonate anions (2,6-NDS) (Figure 2a and 2b). Hydrogen bonding takes place between the OH and H_2O molecules of the aluminum polycation and the sulfonate functional groups of the 2,6-NDS anion with O−H···O distances of approximately 2.74−2.92 Å. Four 2,6-NDS anions per unit cell are observed within the $\mathbf{Al_{32}IDA}$ structure with an interatomic distance between neighboring naphthalene rings at approximately 3.4 Å, suggesting additional van der Waals or $\pi-\pi$ interactions may be present in this compound.[37] Interactions between the naphthalene rings are also expected to occur for $\mathbf{Zn_2Al_{32}NTA}$ because the distance between 2,6-NDS molecules is approximately 2.9 Å.

Two additional sulfate molecules per unit cell are also located within the $\mathbf{Al_{32}IDA}$ lattice that can be attributed to the degradation of the 2,6-NDS anion by UV light. The initial breakdown results in the loss of the sulfonate functional group to create an organosulfonate ligand and sulfate anion,[38] whose presence in our solutions was confirmed by mass spectrometry. Although the solutions that resulted in the formation of the $\mathbf{Al_{32}IDA}$ crystals were not intentionally exposed to UV light, they were aged several weeks in clear glass containers, providing enough radiation to cause degradation of the molecule. In addition, the presence of metals, such as colloidal TiO_2 can catalyze photodegradation of organosulfates[39] and potentially the soluble aluminum Keggin polycations could have also played a role in the decomposition of the 2,6-NDS anion.

The void space within $\mathbf{Al_{32}IDA}$ and $\mathbf{Zn_2Al_{32}NTA}$ was calculated as 1255 and 1930 $Å^3$, respectively, and populated with disordered H_2O molecules and chlorine anions. The number of electrons modeled using the PLATON software suggests that the overall formula for $\mathbf{Al_{32}IDA}$ is $[((Al(IDA)H_2O)_2(Al_{30}O_8(OH)_{60}(H_2O)_{22})](2,6\text{-}NDS)_4(SO_4)_2Cl_4(H_2O)_{36}$. Given the slightly larger void space within the $\mathbf{Zn_2Al_{32}NTA}$ compound, the suggested formula based upon X-ray diffraction is $[(Zn(NTA)H_2O)_2(Al(NTA)(\mu_2\text{-}OH)_2)_2(Al_{30}(\mu_2\text{-}OH)_{54}(\mu_3\text{-}OH)_6(\mu_4\text{-}O)_8(H_2O)_{20}](2,6\text{-}NDS)_5(H_2O)_{52}$.

The polyaluminum clusters present in the $\mathbf{Zn_2Al_{32}NTA}$ and $\mathbf{Al_{32}IDA}$ compounds contain similar structural features as the previously reported $Al_{32}-S$[32] and the W_2Al_{28}[42] molecules. The $Al_{32}-S$ cluster reported by Sun et al.[32] contains Al_{32} clusters that are composed of the Al_{30} molecule with two additional Al atoms bonded to opposite sides of the central belt region in a bridging bidentate fashion. No additional organic ligands are present as chelating agents in the $Al_{32}-S$ compound, but the cluster does contain an additional sulfate anion bonded in a monodentate fashion to the outer Al polyhedra. The W_2Al_{28} cluster contains two additional $(W(VI)O)_6$ groups that replace the capping $Al(O)_6$ polyhedra within the central belt region of the Al_{30} molecule.[42] Until the current study, the $Al_{32}-S$ was the largest polyaluminum cation reported in the literature, but the presence of four additional metal cations bonded to the surface of the Al_{30} cluster in $\mathbf{Zn_2Al_{32}NTA}$ now represents the largest molecule within this class of compounds.

dx.doi.org/10.1021/ic400321k | Inorg. Chem. 2013, 52, 5991−5999

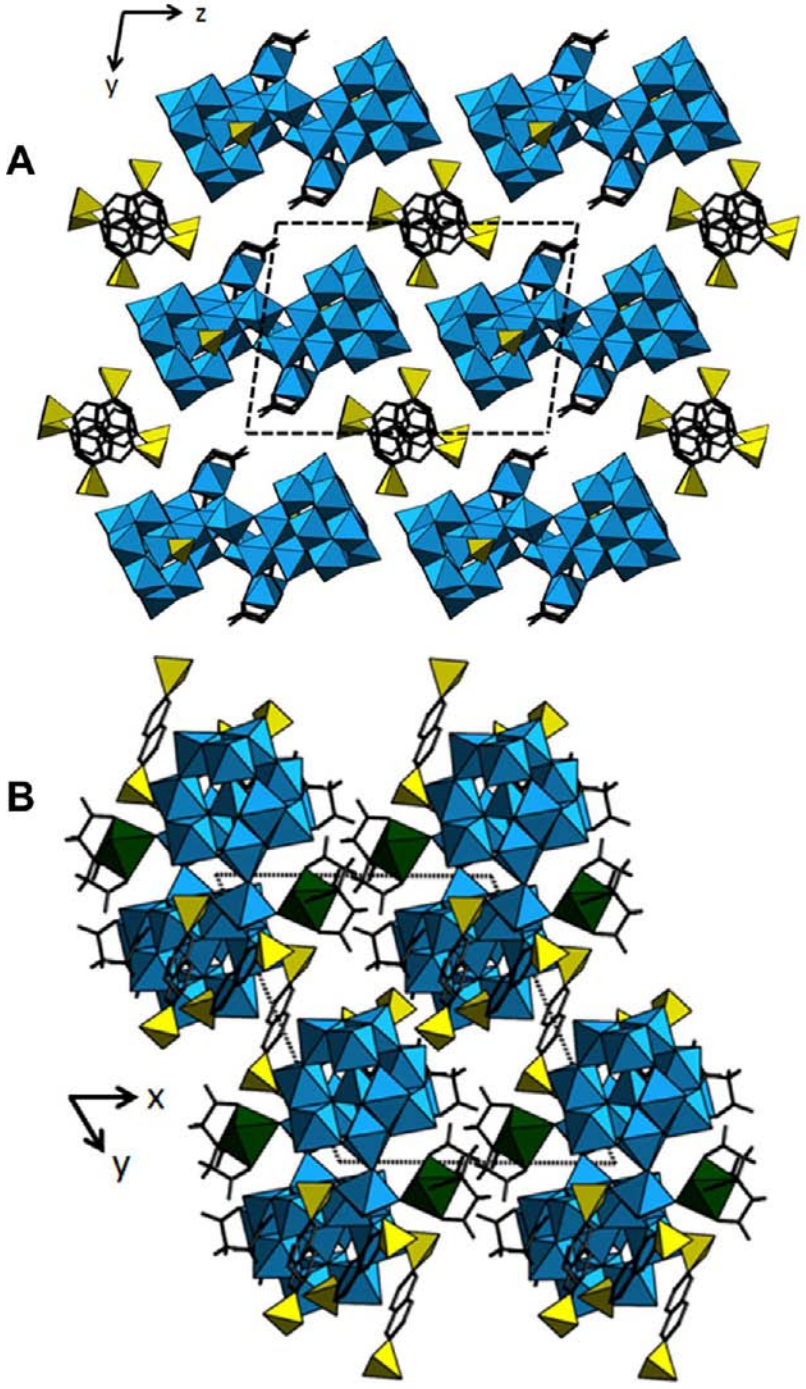

Figure 2. Al_{32}**IDA** (A) and Zn_2Al_{32}**NTA** (B) clusters are linked into a three-dimensional structure through hydrogen bonding with disulfonate anions (yellow polyhedra) and disordered water groups (not-shown).

Infrared Spectroscopy. Infrared spectroscopy was performed on the Al_{32}**IDA** sample to confirm the major structural components of the compound (Figure 3a). The aluminum polycation can be positively identified by the AlO_4 symmetry stretching vibration that is observed at 777 cm^{-1}, as a similar vibrational band is observed on the ε-Al_{13} chorohydrate structure at 780 cm^{-1}.[40] Octahedrally coordinated aluminum atoms are identified via the O−H stretching frequencies associated with the hydroxyl groups on the aluminum polycations. Hydroxyl groups bonded to the aluminum atoms generally occur at lower wavenumbers (2500−3100 cm^{-1}) than observed for molecular water (2900−4000 cm^{-1}), which was also observed in the spectrum.[40] The broad peak present from 2500 to 4000 cm^{-1} indicates the presence of octahedrally coordinated aluminum atoms and disordered solvent (H_2O) molecules. Molecular water present in the structure is also confirmed by the large peak at 1640 cm^{-1} associated with the H_2O bending mode.

Peaks at 1210, 1330, and 1410 cm^{-1} correspond to the C−O, C−N, and C═O stretching of the deprotonated IDA molecule, respectively, and match well with previously reported values.[41] A peak at 1715 cm^{-1} associated with the −COOH functional group is absent in the infrared spectrum of Al_{32}**IDA**, indicating that the IDA molecule is indeed deprotonated and complexed

dx.doi.org/10.1021/ic400321k | *Inorg. Chem.* 2013, 52, 5991−5999

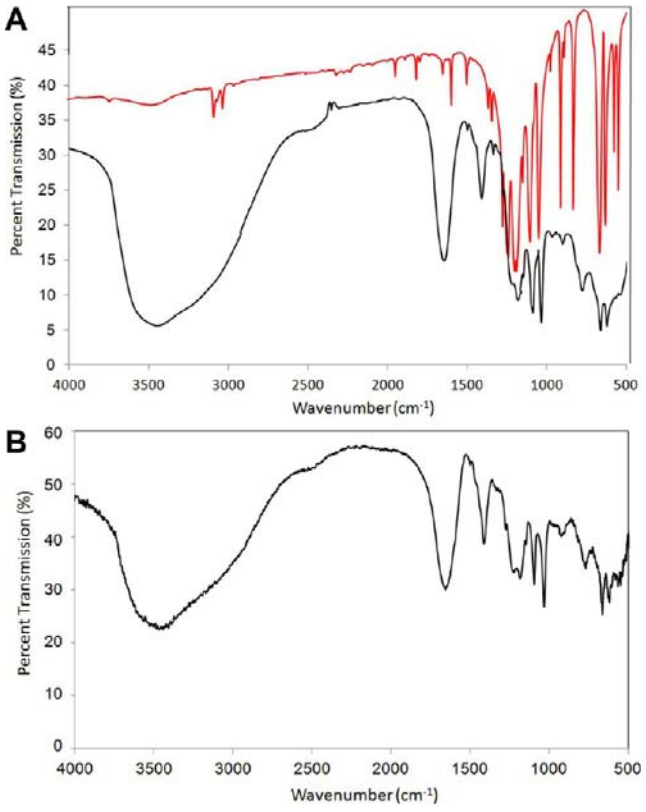

Figure 3. (A) Infrared spectrum of Al_{32}**IDA** (black) confirms the presence of the Keggin-type aluminum polycation, H_2O, and IDA molecule within the compound. The vibrational frequencies associated with the 2,6-NDS molecule can be determined by comparison with the Na_2(2,6-NDS) salt (red). (B) A similar IR spectra is observed for the Zn_2Al_{32}**NTA** compound.

with the metal ligand.[41] The ν(NH) absorption band in the IDA molecule is generally located at 3099 cm^{-1}, but is not observable because of the strength of the O−H vibrational modes. The remainder of the unidentified peaks in the spectrum of Al_{32}**IDA** correspond with vibrations from the 2,6-NDS molecule. A variety of C−C, C−H, S−O frequencies are observed for the 2,6-NDS molecule, as confirmed by the IR spectrum of Na_2(2,6-NDS) (Figure 3a). Peaks associated with the sulfate anion and the sulfonate functional group overlap and cannot be delineated in the spectrum.

Similar vibrational modes are observed for the Zn_2Al_{32}**NTA** compound with large peaks (3900−3600 cm^{-1} and 1635 cm^{-1}) associated with solvent water molecules and the hydroxyl groups on the polyaluminum cluster (Figure 3b). Complexation of the NTA molecule by Zn^{2+} and Al^{3+} cations results in a shift of the peak associated with the carboxylic group from approximately 1715 cm^{-1} to 1639 cm^{-1}. Additional vibrational modes at 1404 cm^{-1} and between 1000 and 1300 cm^{-1} are associated with the carboxylate group on the NTA ligand and disulfonate anions, respectively.

Chemical Composition. The chemical compositions of Al_{32}**IDA** and Zn_2Al_{32}**NTA** were evaluated by scanning electron microscopy equipped with energy dispersive spectroscopy (see Supporting Information, Figure S1). Major peaks in the spectra of Al_{32}**IDA** included Al, O, and S, and a peak associated with Cl was also observed. Similar elements were found in the Zn_2Al_{32}**NTA** compound, and a small peak associated with Zn could also be identified in the spectrum. To confirm the presence of Zn in this compound, a small amount of the sample was dissolved in a weak acid and analyzed with ICP-OES. The expected value of 5.82 ppm agrees with the experimental value of 6.11 ± 0.22 ppm.

Thermogravimetric Analysis. Al_{32}**IDA** was subjected to thermogravimetric analysis to quantify the number of solvent waters present within the structure (Figure 4a). A weight loss of

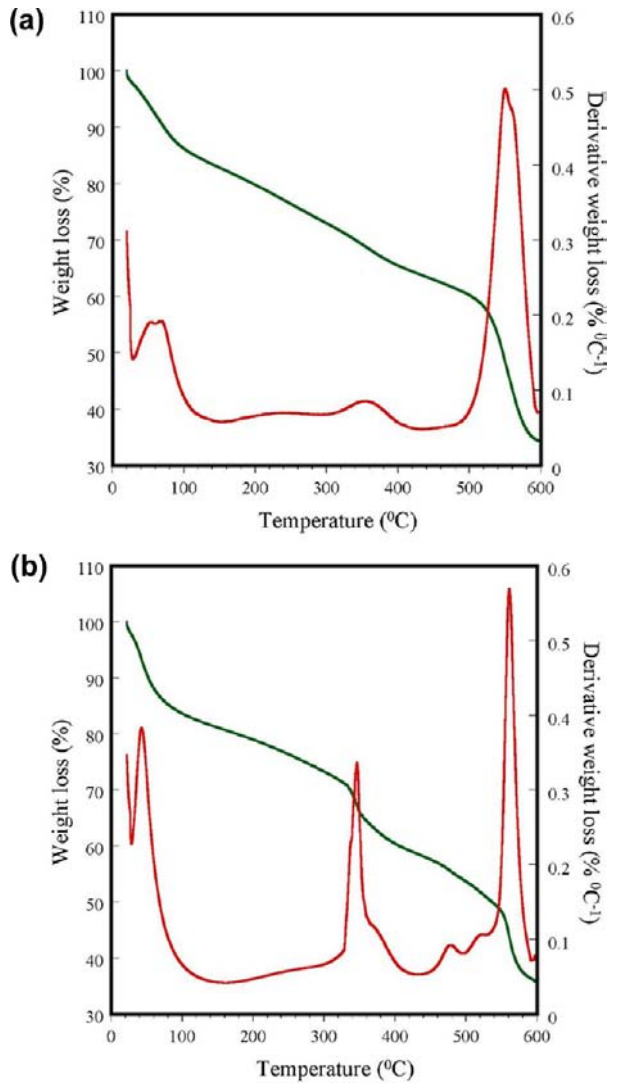

Figure 4. Thermogravimetric analysis of Al_{32}**IDA** (a) and Zn_2Al_{32}**NTA** (b) indicates weight loss because of the removal of the water, organic chelating agents, and the 2,6-NDS crystallization agent. The residual materials in both samples were determined to be an amorphous aluminum oxide or oxyhydroxide by powder X-ray diffraction.

14.64% was observed between 80−120 °C, which accounts for 40 molecules of solvent waters per formula unit. This value is comparable to the 36 water molecules observed using X-ray diffraction and gives an overall formula of $[(Al(IDA)H_2O)_2$-$(Al_{30}O_8(OH)_{60}(H_2O)_{22})](2,6\text{-NDS})_4(SO_4)_2Cl_4(H_2O)_{40}$. Final theoretical and experimental weight losses are relatively consistent at approximately 30%, but loss of the individual chemical components were difficult to delineate within the data. Water molecules associated with the Al^{3+} cations on the cluster are more tightly bound and are expected to be removed at higher temperatures (150−300 °C). For the Al_{32}**IDA**

dx.doi.org/10.1021/ic400321k | Inorg. Chem. 2013, 52, 5991−5999

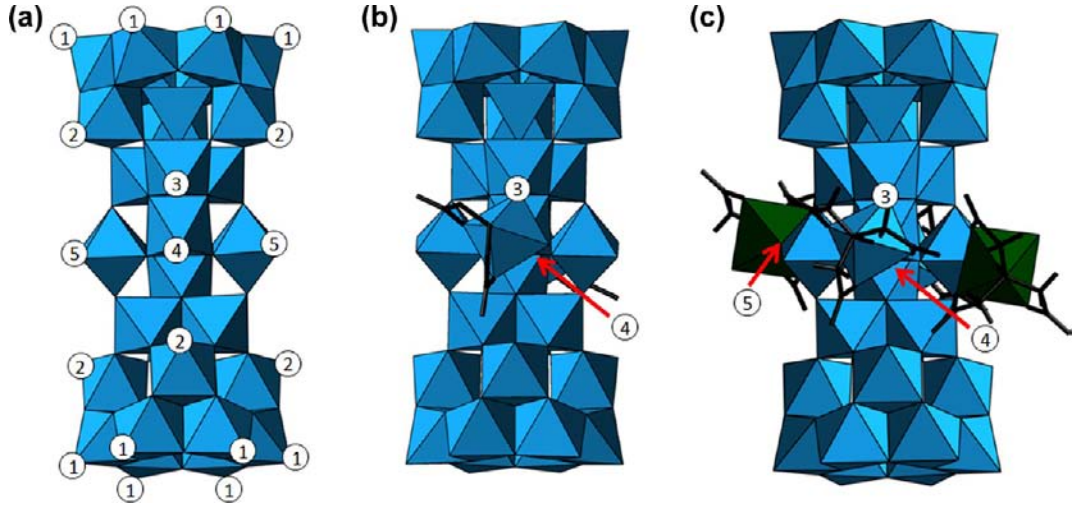

Figure 5. (a) Theoretical studies of the reactivity of the Al_{30} polycation were performed by Rustad, 2005, who differentiated the different water groups associated with the cluster by proximity to the central belt region of the cluster. (b) The 3 and 4 sites are expected to be the most reactive, which agrees with the placement of the chelated Al^{3+} polyhedra on the **Al_{32}IDA** molecule. (c) After deprotonation of the 3 and 4 sites, group 5 is expected to be the most reactive and is corroborated by the observed binding site for the Zn^{2+} metal species in **Zn_2Al_{32}NTA**.

compound, the experimental loss within this region was approximately 12.35%, but the expected value was 11.431%. Loss of the IDA chelator is expected to occur between 300 and 400 °C, but no sharp mass loss or peak in the derivative weight loss was observed within this temperature range. The 2,6-NDS molecules decompose at 550 °C, liberating CO_2, H_2O, and SO_x in the process. The residual weight loss of the compound suggests that our product is an aluminum oxide material, but powder X-ray diffraction indicated that material is amorphous.

Zn_2Al_{32}NTA also contains disordered solvent molecules in the interstitial regions of the lattice that can be observed with the weight loss between 25 and 100 °C (Figure 4b). This weight loss indicates that there are 64 water molecules per formula unit, which is higher than the expected 52 from the single crystal X-ray diffraction data. Gradual weight loss between 100 and 300 °C indicates the loss of water from the aluminum polycation, and a secondary weight loss associated with the decomposition of the NTA chelator occurs at 350 °C. Decomposition of 2,6-NDS is again observed at 550 °C, and the final weight percentage suggests the presence of 2 mols of Zn^{2+}, 2 mols of SO_4^{2-}, and 32 mols of AlOOH per mole of the material. The residual compound may have an empirical formula of $[\mathbf{Zn_{0.07}(AlOOH)(SO_4)_{0.07}}]$, but is also amorphous based upon the powder X-ray diffraction pattern of the heated material.

Surface Modification of Clusters. The specific binding sites for the Al^{3+} and Zn^{2+} atoms on the surface of the Al_{30} polyaluminum cation in the **Zn_2Al_{32}NTA** and **Al_{32}IDA** compounds relate well to the predicted reactivity based upon molecular dynamics simulations of the cluster in an aqueous perchlorate solution.[26] Rustad delineated 26 reactive water molecules of the cluster into five groups in order of increasing proximity to the central belt region (Figure 5a).[26] The most acidic group on the Al_{30} cluster was found to be group 4, which corresponds to the water groups located at the nonbridging site of the δ-Al_{13} capping unit. Molecular dynamics simulations indicated that removal of H atoms occurred even when no additional hydroxide ions were added (pH = 5.5), suggesting that the site is 90% deprotonated and possesses a 16+ charge in a slightly acidic aqueous solution.[26]

Interestingly, group 3 (the nonbridging site of the underlying δ-Al_{13} unit) and 4 are closely associated and will initially form paired $H_3O_2^-$ ligands upon initial deprotonation of group 4. Rustad observed that as the concentration of hydroxyl ion increases, the shared proton moves slightly from the 3 site to the 4 site and the sum of the deprotonated fractions of sites 3 and 4 are nearly constant, suggesting strong coupling of these sites.[26] The chelated Al polyhedra in both **Zn_2Al_{32}NTA** and **Al_{32}IDA** are adsorbed to the surface of the Al_{30} cluster by a bridging bidentate attachment at the 3 and 4 sites (Figure 5b and 5c). Deprotonation of group 4 may result in additional reactivity of group 3, favoring a bridging bidentate coordination to the Al_{30} molecule by metal cations.

These results also suggest that this site may experience some steric and exchange constraints that may determine the type of inorganic or organic species that can adsorb to the surface of the Al_{30} molecule at the 3 and 4 site. The two hydroxyl groups at this position are approximately 2.7 Å apart, which may hinder the adsorption of small organic molecules that do not have the proper bite angle. Instead, the small organic ligands may adsorb via an initial attachment to small monomeric species that coexist with the larger Keggin-type species in solution. Monomeric and dimeric species with a 1:1 Al:NTA or IDA ratio have been observed in aqueous solution between a pH of 3−4, and their structure determined using single-crystal X-ray diffraction.[43−45] As the partially hydrolyzed solution contains monomers and larger polyaluminum species, adsorption to the smaller species may be favored, followed by adsorption of the chelated Al polyhedra to the Al_{30} surface. In addition, complexation of the organic species to the surface of the Keggin molecule would require release of the water molecule followed by bond formation to the hydroxyl or carboxylate functional group on the organic species. Oxygen exchange is relatively slow for the Al_{30} molecule and will initially occur on the 5 site (the nonbridging waters on each of the two linking AlO_6 polyhedra) before the 3 and 4 site, again favoring adsorption of the chelated aluminum species.[26]

Rustad also determined that when five hydroxide ions are added to the aqueous solution, deprotonation of the 5 site occurred and an average protonation state of three of the four

dx.doi.org/10.1021/ic400321k | Inorg. Chem. 2013, 52, 5991−5999

water groups was decreased to 1.6.[26] After the addition of two aluminum atoms to the 3 and 4 position, the Zn^{2+} cations of the **Zn_2Al_{32}NTA** cluster attach to the group 5 sites in a monodentate fashion (Figure 5c). Again the bond distance between the 3 + 4 positions in **Zn_2Al_{32}NTA** is 2.7 Å, whereas the O−O distance in the Zn octahedra is slightly longer at 2.9 Å. Potentially, the Zn atoms may preferentially adsorb at the 5 position after deprotonation of the Al_{30} cluster in aqueous solution.

Reactivity of these sites was also analyzed by Rustad using the MuSiC model, which suggested that the hydration state of the H_2O functional groups is the determining factor governing reactivity.[26] Hydration state is defined by the proton saturation index, which combines the number of water molecules accepting and donating hydrogen bonds from the particular surface function groups. The most acidic groups, the 3 and 4 sites and the 5 position, have the largest proton saturation indices (2.3−2.5) relative to the 1 and 2 sites (2.1−2.2).[26] Therefore the adsorption of metal cations to the surface of the Al_{30} molecule may be predicted by the relative acidity and the hydration state of the surface sites.

While the Al_{30} molecule has many H_2O sites with very different chemical environments, the ε-Al_{13} molecule contains 12 equivalent surface H_2O groups.[26] At a pH >6, deprotonation of the surface H_2O sites of the ε-Al_{13} occur rapidly, concurrent with aggregation and precipitation of the clusters into an amorphous aluminum flocculant.[46] It is difficult to predict where adsorption of metal cations and organic functional groups will occur and indeed there may not be a preferential adsorption site for this molecule. The S−Al_{13} molecule reported by Sun et al., 2011,[35] contains two half-occupied sulfate anions bonded in a monodentate manner to the ε-Al_{13} cluster, suggesting that one sulfate anion can bond to the cluster through a nonbridging H_2O molecule. These results agree with the predicted deprotonation of the Al_{13} molecule, which loses approximately 2.5 total protons over the course of a titration.[46]

These results provide additional information regarding the adsorption of contaminant species by polyaluminum chloride coagulants used in water purification applications, which contain large amounts of the ε-Al_{13} or Al_{30} molecules. Coagulants with high concentrations of the Al_{30} molecule will strongly adsorb contaminants at a lower pH range (5.5) to form soluble species before coagulation and precipitation occurs at pH 7−8. This is a different scenario than the one that may exist for the ε-Al_{13} coagulants, where deprotonation of the molecule occurs almost concurrently with coagulation and contaminant removal may be driven more by physical entrapment (sweep-flocculation) than by chemisorption. Understanding the differences in contaminant removal can provide additional insight into the proper usage and application of the different clarifying reagents for the removal of various constituents during water purification processes.

CONCLUSIONS

The synthesis and structure determination of two modified Al_{30} polyaluminum clusters (**Al_{32}IDA** and **Zn_2Al_{32}NTA**) provides a molecular level understanding of the initial adsorption sites for metal atoms on the surface of this Keggin-type species. Adsorption of contaminants is driven by the deprotonation of the surface water molecules, and our experimental models agree with the most reactive sites on the Al_{30} molecule as predicted by molecular dynamic simulations. As steric factors may also contribute to the binding sites for various contaminants, additional synthesis and characterization of novel Keggin-type species to serve as model compounds may provide new information regarding the adsorption process. Understanding these features can provide additional predictive capabilities for contaminant adsorption and mobility in aqueous environmental solutions.

ASSOCIATED CONTENT

Supporting Information

Crystallographic data in CIF format. Further details are given in Tables S.1−S.2 and Figures S1−S2. This material is available free of charge via the Internet at http://pubs.acs.org.

AUTHOR INFORMATION

Corresponding Author

*E-mail: tori-forbes@uiowa.edu.

Notes

The authors declare no competing financial interest.

ACKNOWLEDGMENTS

We thank the University of Iowa Vice President for Research, Mathematics, and Physical Sciences Funding Program and the University of Iowa College of Liberal Arts and Sciences for funding this work. In addition, we thank Dr. Edward Gillan and Nathan Coleman in the Department of Chemistry for use of the FT-IR instrument, Dr. Sarah Larsen and Paul Mueller for assistance with the ICP-OES, and Dr. Jonas Baltrusaitis in the Central Microscopy Facility for training and assistance with the SEM-EDS.

REFERENCES

(1) Trueba, M.; Trasatti, S. P. *Eur. J. Inorg. Chem.* **2005**, 3393−3403.
(2) Yang, Y. M.; Zhao, X. F.; Zhu, Y.; Zhang, F. Z. *Chem. Mater.* **2012**, *24*, 81−87.
(3) Fu, G.; Nazar, L. F.; Bain, A. D. *Chem. Mater.* **1991**, *3*, 602−610.
(4) Brinker, C. J. Schere, G. W. *Sol-Gel Science: The Physics and Chemistry of Sol-Gel Processing*; Academic Press, Inc.: San Diego, CA, 1990.
(5) Ben-Nissan, B. Choi, A. H. Alumina ceramics. In *Bioceramics and Their Clinical Applications*; Kokubo, T., Ed.; Woodhead Publishing Ltd.: Cambridge, U.K., 2008.
(6) Jolivet, J.-P.; Chaneac, C.; Chiche, D.; Cassaignon, S.; Durupthy, O.; Hernandez, J. *C. R. Geosci.* **2011**, *343*, 113−122.
(7) Casey, W. H. *Chem. Rev.* **2006**, *105*, 1−16.
(8) Baes, C. F. Mesmer, R. E. *The hydrolysis of cations*; John Wiley and Sons: New York, 1976.
(9) Johansson, G. *Acta Chem. Scand.* **1960**, *14*, 771−773.
(10) Akitt, J. W.; Farthing, A. *J. Chem. Soc., Dalton Trans.* **1981**, 1624−1628.
(11) Akitt, J. W.; Elders, J. M. *J. Chem. Soc., Faraday Trans. I* **1985**, *81*, 1923−1930.
(12) Rowsell, J.; Nazar, L. F. *J. Am. Chem.Soc.* **2000**, 122.
(13) Allouche, L.; Gerardin, C.; Loiseau, T.; Ferey, G.; Taulelle, F. *Angew. Chem., Int. Ed.* **2000**, *39*, 511−514.
(14) Kim, T. W.; Yoo, H.; Kim, I. Y.; Ha, H. W.; Han, A. R.; Chang, J. S.; Lee, J. S.; Hwang, S. J. *Adv. Funct. Mater.* **2011**, *21*, 2301−2310.
(15) Zhao, S.; Feng, C. H.; Huang, X. N.; Li, B. H.; Niu, J. F.; Shen, Z. Y. *J. Hazard. Mater.* **2012**, *203*, 317−325.
(16) Furrer, G.; Trusch, B.; Muller, C. *Geochim. Cosmochim. Acta* **1992**, *63*, 3068−3076.
(17) Lee, A. P.; Furrer, G.; Casey, W. H. *J. Colloid Interface Sci.* **2002**, *250*, 269−270.
(18) Casey, W. H.; Rustad, J. R.; Banerjee, D.; Furrer, G. *J. Nano. Res* **2005**, *7*, 377−387.

(19) Lothenbach, B.; Furrer, G.; Schulin, R. *Environ. Sci. Technol.* **1997**, *31*, 1452−1462.
(20) Badora, A.; Furrer, G.; Grunwald, A.; Schulin, R. *J. Soil Contam.* **1998**, *7*, 573−588.
(21) Mertens, J.; Casentini, B.; Masion, A.; Pothig, R.; Wehrli, B.; Furrer, G. *Water Res.* **2012**, *46*, 53−62.
(22) Dubbin, W. E.; Sposito, G. *Environ. Sci. Technol.* **2005**, *39*, 2509−2514.
(23) Stewart, T. A.; Trudell, D. E.; Alam, T. M.; Ohlin, C. A.; Lawler, C.; Casey, W. H.; Jett, S.; Nyman, M. *Environ. Sci. Technol.* **2009**, *43*, 5416−5422.
(24) Masion, A.; Vilge-Ritter, A.; Rose, J.; Stone, W. E. E.; Teppen, B. J.; Rybacki, D.; Bottero, J. Y. *Environ. Sci. Technol.* **2000**, *34*, 3242−3246.
(25) Xiaoying, M.; Guangming, Z.; Chang, Z.; Zisong, W.; Jian, Y.; Jianbing, L.; Guohe, H.; Hongliang, L. *J. Colloid Interface Sci.* **2009**, *337*, 408−413.
(26) Rustad, J. R. *Geochim. Cosmochim. Acta* **2005**, *60*, 4397−4410.
(27) Hoft, R. W. W. *COLLECT*; Nonius B. V.: Delft, The Netherlands, 1998.
(28) Otwinoswki, Z.; Minor, W. *Macromolecular Crystallography*, Methods in Enzymology; Carter, C. W., Sweet, R.M. Eds.; Academic Press: New York, 1997.
(29) Sheldrick, G. M. *Acta Crystallogr., Sect. A* **2008**, *64*, 112−122.
(30) International Union of Crystallography. *International Tables of Crystallography*; Wiley Publications: Oxford, England, 2006.
(31) Spek, A. L. *J. Appl. Crystallogr.* **2005**, *36*, 7−13.
(32) Sun, Z.; Wang, H.; Tong, H.; Sun, S. *Inorg. Chem.* **2011**, *50*, 559−564.
(33) Johansson, G.; Lungren, G.; Sillen, L. G. *Acta Chem. Scand.* **1963**, *14*, 769−771.
(34) Mainicheva, E. A.; Gerasko, O. A.; Sheludyakova, L. A.; Naumov, D. Y.; Naumova, M. I.; Fedin, V. P. *Russ. Chem. Bull., Int. Ed.* **2006**, *55* (2), 267−275.
(35) Drljaca, A.; Hardie, M. J.; Raston, C. L. *J. Chem. Soc., Dalton Trans.* **1999**, 3639−3642.
(36) Abeysinghe, S.; Unruh, D. K.; Forbes, T. Z. *Cryst. Growth Des.* **2012**, *12*, 2044−2051.
(37) Grimme, S. *Angew. Chem., Int. Ed.* **2008**, *47*, 3430−3434.
(38) Nielson, A. H..Allard, A.-S. *Organic Chemicals in the Enviornment Mechanisms of Degradation and Transformation*; CRC Press: Boca Raton, FL, 2013.
(39) Szabo-Bardos, E.; Zsilak, Z.; Lenvay, G.; Horvath, O.; Markovics, O.; Hoffer, A.; Toro, N. *J. Phys. Chem. B* **2008**, *112*, 14500−14508.
(40) Teagarden, D. L.; Hem, S. L.; White, J. L. *J. Soc. Cos. Chem.* **1982**, *33*, 281−295.
(41) Kumar, G.; Kiremire, E. M. R. *Chemistry* **2007**, *16*, 387−393.
(42) Son, J. H.; Kwon, Y.-U. *Inorg. Chem.* **2003**, *2003*, 4153−4159.
(43) Yokoyama, T.; Abe, H.; Kurisaki, T.; Wakita, H. *Anal. Sci.* **1999**, *15*, 393−395.
(44) Kilyen, M.; Lakatos, A.; Latajka, R.; Labadi, I.; Salifoglou, A.; Raptopoulou, C. P.; Kozlowski, H.; Kiss, T. *J. Chem. Soc., Dalton Trans.* **2002**, 3578−3586.
(45) Dubey, S. N.; Singh, A.; Puri, D. M. *J. Inorg. Nucl. Chem.* **1981**, *43*, 407−409.
(46) Furrer, G.; Ludwig, C.; Schindler, P. W. *J. Colloid Interface Sci.* **1992**, *149*, 56−67.